

Study on electrical and magnetic properties of structural ordering of double Perovskite material.

***B. Jaya Prakash¹ K. Srinivasa Rao² D. Venkata Siva Reddy³ & B. Srikanth⁴**

¹*Department of Physics, B.T G College, Madanapalli-517325, A.P., INDIA.*

^{2&4}*Department of Physics, Government Degree College, Mandapeta -533308, , A.P., INDIA.*

³*Department of Computer Science, B.T GCollege, Madanapalli-517325, A.P., INDIA.*

Abstract:

Understanding and realization of Multiferroic materials properties at room temperature are gained significant importance in recent days for advance in multifunction devices. Suitable selection and process of the materials are very important prerequisite for development of multiferroic properties in the materials for the multifunction devices applications. In addition to multifunctional spintronics devices applications, these multiferroic materials used for smaller, faster and energy efficient data storage which is huge demand of future technology.

In present study, to enhance the multiferroic properties with strong coupling double perovskite structure $\text{Bi}_2\text{NiMnO}_6$ is considered under study. This composites gained significant importance with low leaking current and shows both ferromagnetic transition temperature $T_{\text{CM}}=144$ K and ferroelectric ferroelectric transition temperature $T_{\text{CE}}=485$ K properties. $\text{Bi}_2\text{NiMnO}_6$ shows large moment of ferromagnetically coupled Ni and Mn spins. In the present work, double perovskite $\text{Bi}_2\text{NiMnO}_6$ nanoparticles are prepared by chemical co-precipitation method and are studied, thermal, magnetic, electrical properties systematically in order to identify its suitability for suitability in devices applications.

Key words: Strong coupling, Multifunctional & Double Perovskite structure

INTRODUCTION:

Coexistence existences of ferroelectric, magnetic orderings and ferroelastic have been attracting immense interest in recent days due to their interesting fundamental nature exhibited together. Existence of primary ferroic order in a material opens the development of new kind of multifunctional devices, which leads to further miniaturization of devices with more efficiency. Potential multifunctional materials have the wide range of application in the areas such as spintronics devices, microelectronic devices, storage devices, quantum devices and sensors as a multifunctional devices. Due to immense wide range of applications of multiferroic materials are gained significant importance theoretically as well as experimentally [1-2]. Multiferroic materials have the ability to control and tunability between the ferroic orders with three degrees of freedom. However, despite their potential usefulness, multiferroic materials are rare in nature and none of them have been used in practical applications so far due to their small response to an external field [3-4]. At present, room temperature based multiferroic materials with strong coupling between ferroic orders are required for fabricating multifunctional devices [5-6].

In double perovskites have two different transition metal cations at the B-sites of its perovskite structure and these transition metal cations provides necessary delocalized d orbital gives rise to extraordinary magnetic properties. And structural ordering of the double perovskites used give the ferroic ordering with the material. In present study, perovskite structure $\text{Bi}_2\text{NiMnO}_6$ (BNMO) is adopted for present study. This composite gained significant importance with low leakage current and shows both ferromagnetic transition temperature $T_{\text{CM}} 144 \text{ K}$ and ferroelectric transition temperature $T_{\text{CE}} 485 \text{ K}$ properties [7]. $\text{Bi}_2\text{NiMnO}_6$ shows large moment of ferromagnetically coupled Ni and Mn spins. In the present work, double perovskite $\text{Bi}_2\text{NiMnO}_6$ nanoparticles are prepared by chemical co-precipitation method and are studied,

thermal, magnetic, electrical properties systematically in order to identify its suitability for multifunctional devices applications [8-9].

EXPERIMENTAL

Stoichiometric amount of $\text{Bi}(\text{NO}_3)_3$ (99.9%) AR grade (SRL chemicals) was dissolved in distilled water (100 ml) and $\text{Mn}(\text{NO}_3)_2 + \text{NiCl}_2$ was dissolved in distilled water (100 ml). Then solutions of $\text{Bi}(\text{NO}_3)_3$ and $\text{Mn}(\text{NO}_3)_2 + \text{NiCl}_2$ were mixed homogeneously by using a magnetic stirrer 24hrs. Then sodium hydroxide (NaOH) added to the above solution drop by drop with a constant stirring of the above solution mixture to have the pH value > 10 in order to ensure upon a complete precipitation. After filtering, the precipitate was washed for several times using distilled water and later it was dried in an oven at 100°C for 24 hrs. As received precipitation used for measuring differential thermal analysis (DTA) and thermo gravimetric analysis (TGA) simultaneously in nitrogen (N_2) atmosphere at a heating rate of $10^\circ\text{C}/\text{min}$. on a Netzsch STA 449F1 simultaneous thermal analyzer. Based on the weight losses of volatile molecules in the sample from the TG graph, the samples were sintered at 500°C , 600°C and 700°C , for 5 hrs. According measurement of TG-DTA the existing of exothermic, endothermic and crystalline temperatures samples are sintered at 400°C , 500°C , 600°C and 700°C with controlled temperature raising and cooling with $5^\circ\text{C}/\text{minute}$. Nanoparticles sintered at 400°C are pressed into circular pellets with 14 mm diameter and approximately 2 mm thickness by applying pressure $180\text{Kg}/\text{Cm}$. From the different sintering temperatures, optimization of the sintering temperature of the sample for this sample characterized with different characterization techniques in order to understand the multiferroic nature of the material.

RESULTS AND ANALYSIS

TG-DTA analysis

Simultaneous measurement of TGA-DTA allows both heat flow and weight changes (TGA) in $\text{Bi}_2\text{NiMnO}_6$ sample as a function of temperature in a controlled nitrogen (N_2) atmosphere as shown in Fig.1.

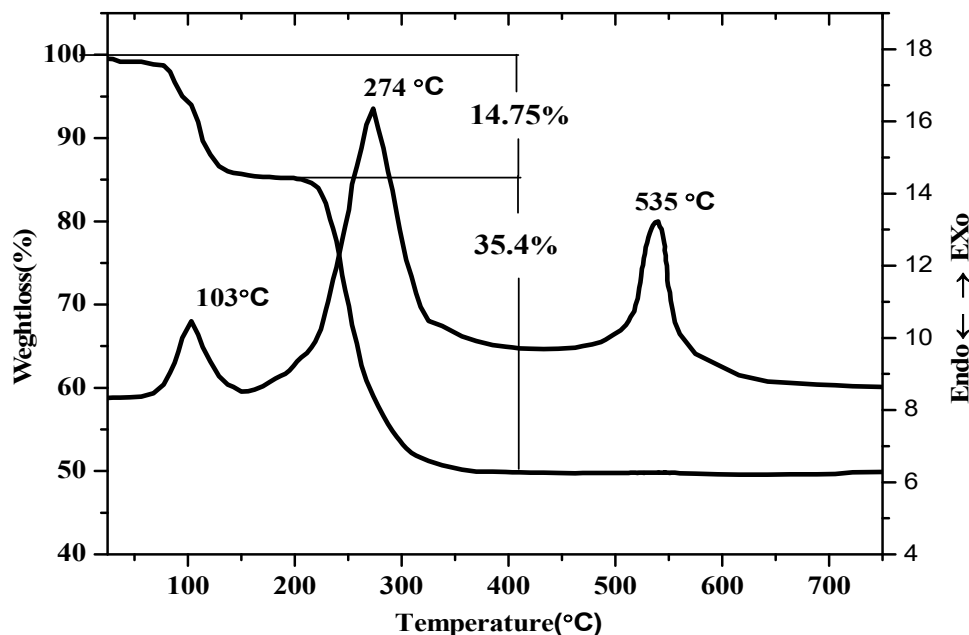


Fig.1. TG-DTA profiles of as synthesized of $\text{Bi}_2\text{NiMnO}_6$ nanoparticles.

TG measurement clearly shows the thermal decomposition process which in turn facilitates estimation of sample structures and compositions. The complementary information obtained allows differentiation between endothermic and exothermic events with no associated weight loss (melting and crystallization) and those involve a weight loss [10-11]. The TG profile shows the weight loss of the sample in two step process in the temperature range of 30 °C -750 °C and the initial mass of sample is 58.46 mg. The initial and major weight loss of the sample take place between 28 °C - 150 °C and the observed weight loss is 8.62 mg (14.75%), this weight loss corresponds to the evaporation of water, residual solvent, combustion of organic species and decomposition of oxalate group, respectively. DTA analysis shows one endothermic peak at 103°C

within the temperature range 30 °C- 150 °C. The occurrence of endothermic peaks in the temperature range, the magnitude of which depends on the synthesis method carried out. An endothermic peak at 103 °C corresponds to the phase change of the sample from semi solid phase to solid phase, for TG-DTA measurement and that peak may be due to the evaporation of water and combustion of organic species. The second weight loss has been noticed in the range 150 °C- 400 °C is equal to 20.69 mg (35.4%) due to the combustion of remaining intermediate oxalate, loss of carbonates and hydrogen, respectively. In the temperature range of 150 °C - 400°C, DTA curve shows endothermic peaks at 274 °C is due to combustion of intermediate oxalates, loss of carbonates and other spices. Between 400-750°C, there is no the weight loss of sample, exothermic peak at 535 °C indicate the ordering of crystallization process [12-13] it also observed from XRD profiles to change from semi-crystalline to a pure crystalline structure. When the weight loss of the sample becomes constant that means all volatiles and impurities are removed the required sample is formed. All details of the TG-DTA profiles of Bi₂NiMnO₆ are tabulated here:

Table.1. TG-DTA profiles of Bi₂NiMnO₆ nanoparticles

| Temperature range | TGA Profile | | DTA Profile | |
|--|--|-----------------|------------------|-------------------|
| | Initial weight of the sample: 58.46 mg | | Exothermic (°C) | Endothermic (°C) |
| | Weight loss (%) | Weight loss(mg) | | |
| 30 °C - 150 °C | 14.75 | 8.62 | 103 | - |
| 150 °C-400 °C | 35.4 | 20.69 | 274 | - |
| 400 °C-750 °C | Constant | Constant | 535 | - |
| Residual weight of the sample at 750 °C: 29.15 mg, | | | | |

XRD analysis

Based on the weight loss of the sample from thermo gravimetry analysis (TGA), the major weight loss of the sample occurs between from 30 - 650 °C and above 650 °C weight loss of the sample is small thus indicating the formation of the pure $\text{Bi}_2\text{NiMnO}_6$. X-ray diffraction profiles of the $\text{Bi}_2\text{NiMnO}_6$ nanoparticles are sintered at 500 °C, 600 °C and 700 °C temperature as shown in Fig.2. The Crystallinity of the $\text{Bi}_2\text{NiMnO}_6$ sintered below 500 °C is partially crystalline nature and amorphous natured and it is evidenced by the DTA curve.

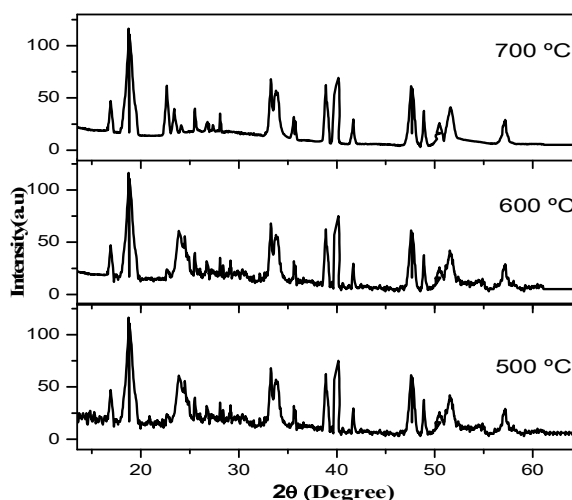


Fig.2. XRD profiles of $\text{Bi}_2\text{NiMnO}_6$ nanoparticles sintered at different temperatures.

On sintering $\text{Bi}_2\text{NiMnO}_6$ nanoparticles the crystallinity is improved from 500 °C - 700 °C and among these profiles the optimized temperature 700 °C and these peaks are well matched with refined XRD Structure. The XRD pattern of $\text{Bi}_2\text{NiMnO}_6$ nanoparticles have crystallized in the monoclinic structure with space group $C121$ and lattice parameters are $a=9.527 \text{ \AA}$, $b=5.431 \text{ \AA}$ and $c=9.552 \text{ \AA}$. From XRD profile, the sample sintered at 700 °C has sharp peaks reveal the highly crystalline nature of $\text{Bi}_2\text{NiMnO}_6$ nanoparticles. The impurity peaks are attributed to a small amount of Mn_3O_4 . [14-15]. Sample sintered at 500 °C show crystalline broad crystalline peaks represent particles are in nano size and further increasing of sintering temperature impurities peaks are reduced at 700 °C which indicates formation of the pure single phase $\text{Bi}_2\text{NiMnO}_6$.

nanoparticles. The average crystallinity size is calculated from Scherrer's formula ($t = K\lambda / (B\cos\theta_B)$), where t is the average size of the particles, assuming particles to be spherical, $K = 0.9$, λ ($=1.5406 \text{ \AA}$) is the wavelength of X-ray radiation, B is the full width at half maximum of the diffracted peak and θ_B is the angle of diffraction [16]. The average crystallite of the $\text{Bi}_2\text{NiMnO}_6$ at different sintering temperatures tabulated below.

Table.2. Variation of crystallinity size with sintering temperature of $\text{Bi}_2\text{NiMnO}_6$

| Sintering temperature ($^{\circ}\text{C}$) | 2 θ position (Degrees) | Full width at half Maximum B (radians) | Average crystallinity size (nm) |
|--|-------------------------------|--|---------------------------------|
| 500 | 18.7 | 0.35 | 40 |
| 600 | 18.7 | 0.32 | 44 |
| 700 | 18.7 | 0.3 | 46 |

SEM analysis

Fig.3. shows SEM images revealing the morphology of the $\text{Bi}_2\text{NiMnO}_6$ nanoparticles, sintered at 500°C , 600°C & 700°C . Systematic study of the microscopy reveals the sample sintered at 500°C shows the porous and loosely packed grains in microscopy. $\text{Bi}_2\text{NiMnO}_6$ nanoparticles sintered at 600°C shows the grains are appear to be like spherical shape with non uniform in size and the average grain sizes are in nm range. Upon increasing the temperature the grains sizes are continuously increasing the with overlapping of the spherical grain boundaries are appear and grain boundaries are boundaries are completely to each other at 700°C shows grain overlapped to each other and densely packed microscopy is observed. Also, an increase in the grain size with increase in the sintering temperature is noticed. From Sem. profile the optimized sintering temperature is 700°C for 5hrs to controlled the grain size [17-18]

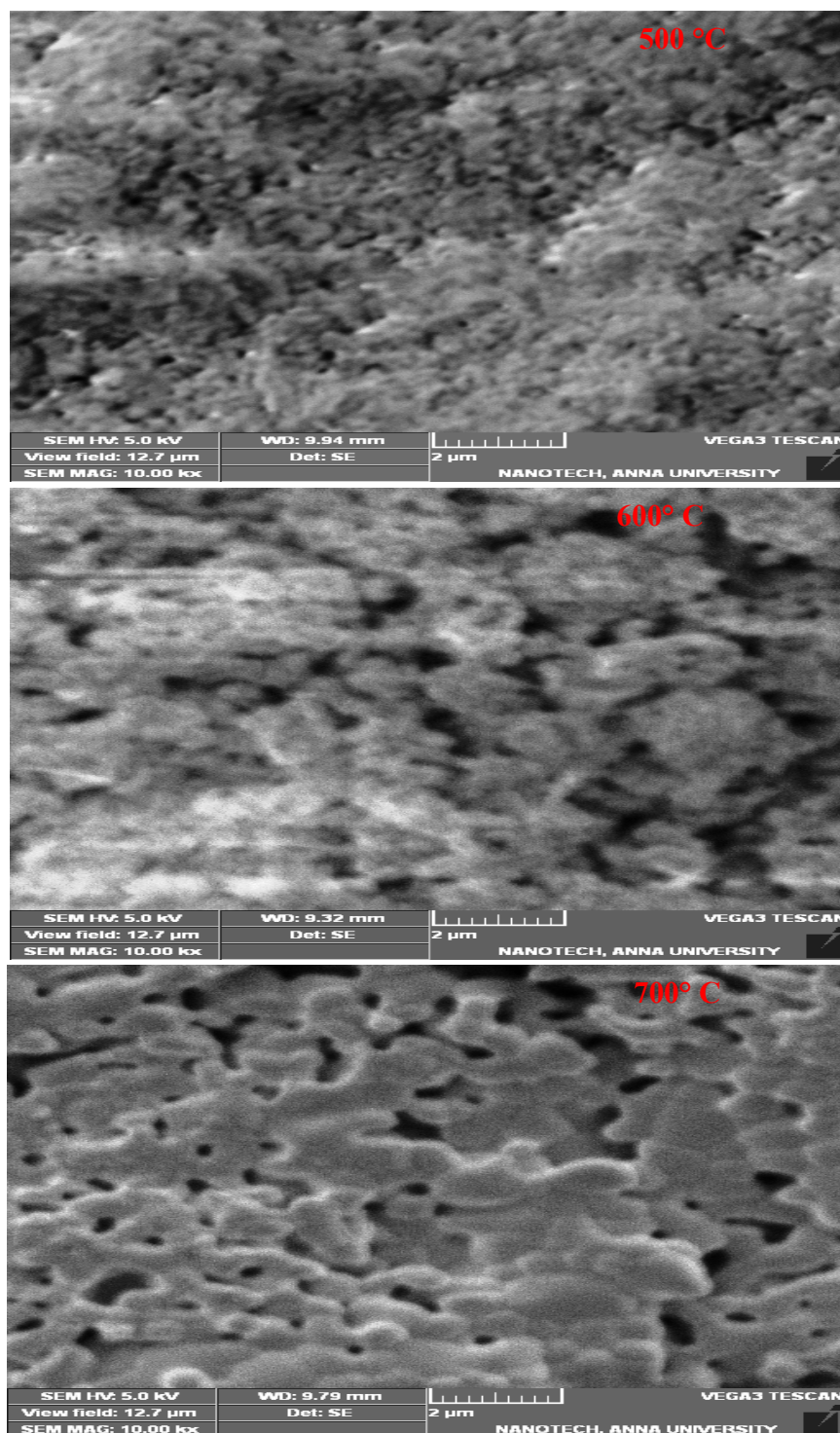


Fig.3. SEM images of $\text{Bi}_2\text{NiMnO}_6$ nanoparticles at 500 °C, 600 °C & 700 °C

From SEM images of the sample observed that grain sizes are not in the uniform size and shape. The approximate average grain size of the $\text{Bi}_2\text{NiMnO}_6$ values with sintering temperature shown in Fig. 4.

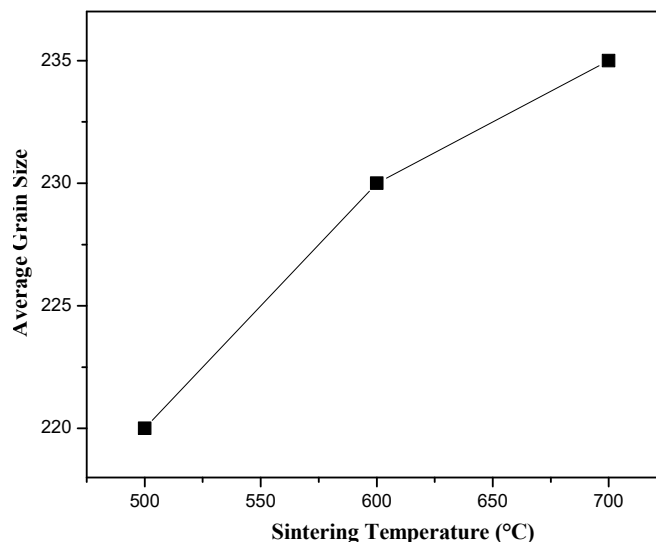


Fig.4. Variation of average grain size with sintering temperatures

FTIR analysis

For identifying the functional groups of $\text{Bi}_2\text{NiMnO}_6$ nanoparticles, FTIR spectrum is as shown in **Fig.5**. The bands at 529 cm^{-1} and 609 cm^{-1} related to the Mn-O or Bi-O inorganic network and octahedral coordinated BiO_6 ; Bi-O stretching and bending vibrations are expected between $500\text{-}700\text{ cm}^{-1}$. In Tetrahedral coordinated BiO_4 , Bi-O stretching and bending vibrations are expected between $700\text{-}850\text{ cm}^{-1}$ and it is observed at 810 cm^{-1} [19-20]. The peak at 1024 cm^{-1} is due to characteristic $\text{Mn}^{3+}\text{-O}$ vibrations or may be due to characteristic nitrate NO_3 vibrations because cations are taken in nitrate or may be due to the stretching vibrations of carbon group. The band at 15244 cm^{-1} could be attributed to the absorption bond O-H engaged in ferric hydroxide or Ni-O vibrations mode [21]. The peak at 2364 cm^{-1} is CO_2 symmetric and asymmetric stretching modes of vibrations. The bands observed at 3616 cm^{-1} and 3616 cm^{-1} and 1630 cm^{-1} are

assigned to OH⁻ stretching and H-O-H bending vibrations of structural water. The infrared absorption bands associated with the OH⁻ stretching vibration have earlier been reported [22].

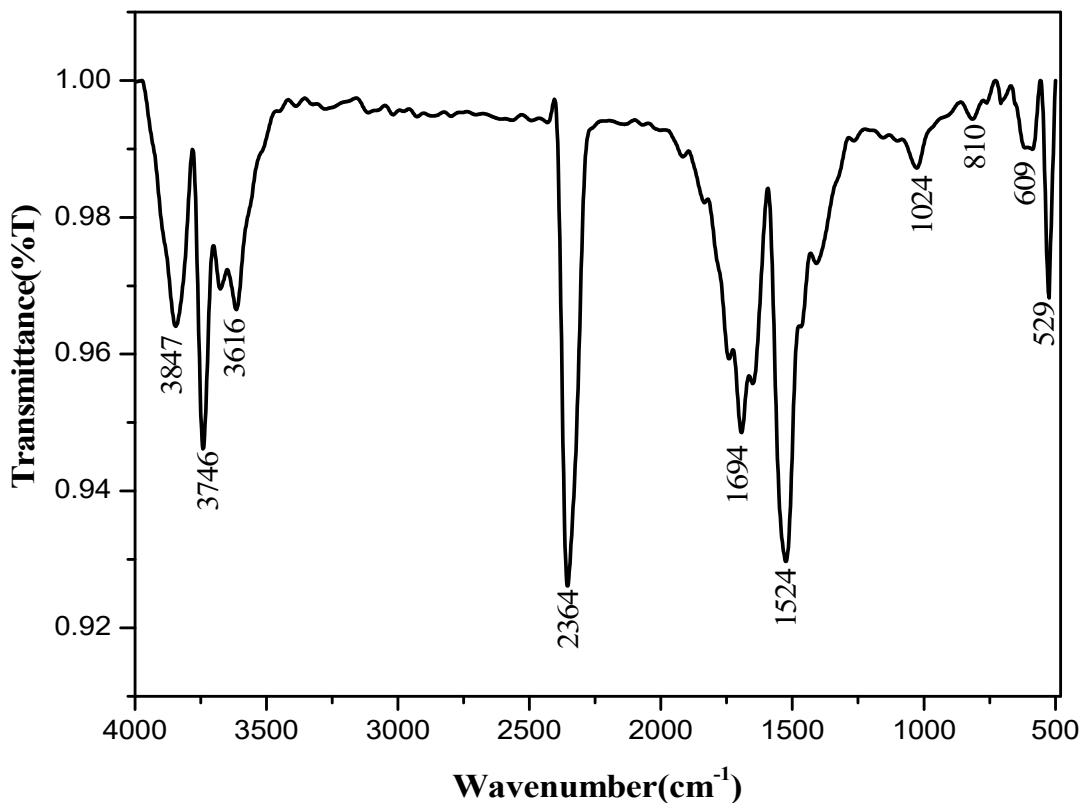


Fig.5. FTIR Spectra of the $\text{Bi}_2\text{NiMnO}_6$ nanoparticles sintered at 700°C

Table.3. Different modes of vibrations of $\text{Bi}_2\text{NiMnO}_6$ nanoparticles

| S.NO | Wavenumber (cm^{-1}) | Modes of Vibrations |
|------|---------------------------------|---|
| 1 | 529 and 609 | Mn-O stretching vibration and O-Mn-O bending vibrations |
| | 810 | Bi-O stretching and bending |
| | 1024 | Mn^{3+} -O vibrations |
| 2 | 1524 | Ni-O stretching and bending |
| 3 | 1380 | NO_3 vibrations |
| 4 | 2364 | CO_2 symmetric and asymmetric stretching modes |
| 5 | 3746, 3616 and 1595 | OH ⁻ stretching and H-O-H bending vibrations |

M-H Hysteresis Loop

Magnetic properties of $\text{Bi}_2\text{NiMnO}_6$ nanoparticles verified by the hysteresis loops of $\text{Bi}_2\text{NiMnO}_6$ nanoparticles recorded at room temperature Fig.6. From the M-H hysteresis loop $\text{Bi}_2\text{NiMnO}_6$ nanoparticles exhibit weak ferromagnetism at room temperature. For $\text{Bi}_2\text{NiMnO}_6$, it is expected that Ni ions present a valence +2 with e_g electrons, while Mn ions present a valence +4 with no e_g electrons. According to the Goodenough Kanamori rules the expectation for magnetic interaction between Ni^{2+} and Mn^{4+} should be ferromagnetic ordering with a linear arrangement of Ni-O-Mn [23]. In case of $\text{Bi}_2\text{NiMnO}_6$ nanoparticles exhibiting two magnetic transitions $T_1=122$ K and $T_2=44$ K [23]. High temperature ferromagnetic transition occurred due to the Ni^{2+} -O- Mn^{4+} super exchange interaction while the low temperature magnetic transition occurred due to the Ni³⁺-O-Mn³⁺ super exchange interaction. Magnetic transitions at $T_2=42$ K also get influenced by impurities phase Mn_3O_4 present in the sample was detected through the XRD profile [23].

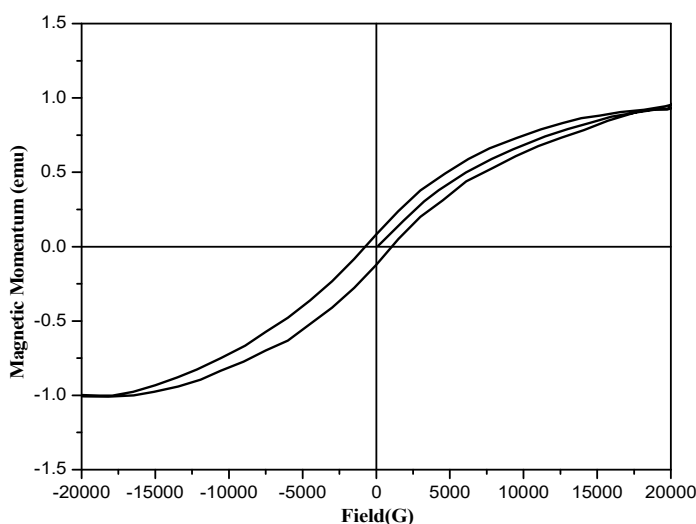


Fig.6. M-H Hysteresis loop of the $\text{Bi}_2\text{NiMnO}_6$ nanoparticles

Ferroelectric properties

Fig.7. $\text{Bi}_2\text{NiMnO}_6$ nanoparticles exhibiting spontaneous polarization causes ferroelectric hysteresis loop at room temperature $\text{Bi}_2\text{NiMnO}_6$. The reason for exhibiting spontaneous polarization of $\text{Bi}_2\text{NiMnO}_6$ nanoparticles is due to hybridization between active $6s^2$ lone pair of Bi^{+3} and oxygen 2p orbital. When Bismuth is Bi^{+3} state the empty 6p orbital of Bi^{+3} energy is closer to energy of oxygen 2p orbital, then hybridization takes place causes Bi^{+3} being displaced within its oxygen surroundings toward anion by breaking center of symmetry causes spontaneous polarization [24]. In addition to order phase possesses $\text{Ni}^{2+}(t_{2g}^6 e_g^2)$ and $\text{Mn}^{4+}(t_{2g}^3 e_g^0)$ different alternating planes leads to large polarization with large dielectric constant. Slight change may occur due to the disordered phase between Ni and Mn cations are distributed in the crystal structure. And also due to small distortion of Ni^{2+} and Mn^{4+} ion in octahedral symmetry with oxygen surrounding cause's spontaneous polarization also contributes to total polarization. Saturation polartzation if found to be $28\mu\text{C}/\text{cm}^2$

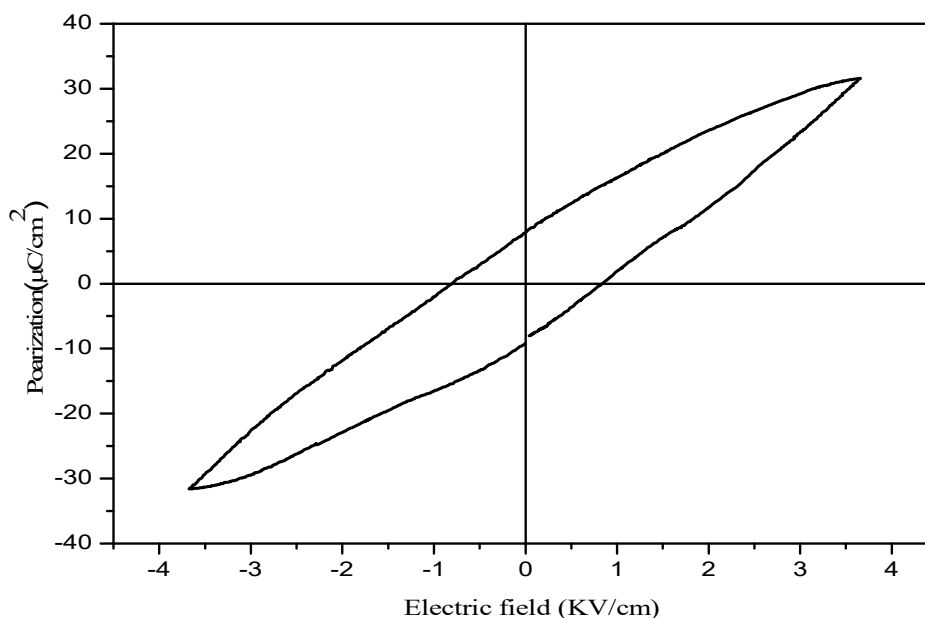


Fig.7. P-E Hysteresis loop of $\text{Bi}_2\text{NiMnO}_6$ nanoparticles sintered at 700°C

CONCLUSION

Double Perovskite $\text{Bi}_2\text{NiMnO}_6$ nanoparticles are prepared by using chemical co-precipitation method and controlled the size of the particles by using the precipitation agent under the optimized conditions. In order to optimize the sintering conditions of the sample based on the TG-DTA profiles of the samples their thermal stability has been understood and from DTA profiles existence of the exothermic, formation of crystalline temperature have been understood and verified with XRD data. From the XRD profiles, the crystalline structure has been identified and average crystalline sizes have also been calculated which nano in size are. $\text{Bi}_2\text{NiMnO}_6$ nanoparticles belongs to monoclinic structure with space group $C121$ and lattice parameters are $a=9.527\text{Å}$, $b=5.431\text{Å}$ and $c=9.552\text{Å}$. The morphology studies based on the sintered temperatures of the samples $\text{Bi}_2\text{NiMnO}_6$ have been understood from the SEM images and whose grain sizes are in the nano range. Grain growth calculated with sintering temperature found to be not uniform growth. The functional groups have been understood from FTIR spectral analysis of $\text{Bi}_2\text{NiMnO}_6$. $\text{Bi}_2\text{NiMnO}_6$ nanoparticles exhibits ferromagnetism at room temperature and ferromagnetic ferromagnetic transition temperature magnetic transitions were observed at $T_1=122\text{ K}$ and $T_2=44\text{ K}$. Two transitions are observed due to purity and impurity phase and Critical temperature at $T_1=122\text{ K}$ pure phase of the sample and $T_2=44\text{ K}$ transition due to impurity phase and these phase observed in XRD Profile. Ferroelectric transition temperature found to be $T_{\text{CE}}=485\text{ K}$ properties and exhibiting room temperature P-E hysteresis loop and saturation polarization is $28\mu\text{C}/\text{cm}^2$. Perovskite structure BiFeO_3 nanoparticles shows weak ferromagnetism ferroelectric properties very weak coupling. But comparing with double perovskite structure $\text{Bi}_2\text{NiMnO}_6$ materials transition temperatures are raised to high temperature and strong coupling existed between ferroic orders compared to other conventional multiferroic materials.

REFERENCES

1. M. A. Jalaja, Soma Dutta, "Ferroelectrics and multiferroics for next generation photovoltaic" Review Article: *Advanced Materials Letters*, 6(7), P. 568-584.
2. R. Ramesh, N.A. Spaldin, Multiferroics: Progress and prospects in thin films, *Nat. Mater.* 2007, 6, 21-29.
3. V. J. Folen, G. T. Rado (1961), "Anisotropy of the Magnetoelectric Effect in Cr_2O_3 ", *Physical Review Letters*, 6, P.607.
4. Hans Schmid (1994), "Multi-ferroic magnetoelectrics", *Ferroelectrics* P.162.
5. C.-Y. Kuo, Z. Hu (2016), "Single-domain multiferroic BiFeO_3 films" *Nature Communications*, 7, 12712.
6. Chu, Y.H (2008), "Electric-field control of local ferromagnetism using a magnetoelectric multiferroic", *Nature Materials*, 7, P. 478–482
7. Y. Du, Z. X. Cheng and X. L. Wang (2011), "Magnetic and ferroelectric properties of multiferroic $\text{Bi}_2\text{NiMnO}_6$ nanoparticles", *Journal of Applied Physics* 109, 07B507.
8. B. Jaya Prakasha, B. H. Rudramadevia (2014), "Analysis of Ferroelectric, Dielectric and Magnetic Properties of GdFeO_3 Nanoparticles", *Ferroelectrics Letters Section*, 41, P. 110–122.
9. Nabil bader, Abdulsalam A. Benkhaya I(2014), "Co-Precipitation as a sample preparation Technique for trace element analysis", *International Journal of Chemical Sciences*, 12(2), P.519-525.
10. V.S. Ramachandran, R. M. Paroli (2002), "Handbook of thermal analysis of construction materials, Noyes Publications", Norwich, New York.
11. J. Li & T. Qiu (2011), "Synthesis of SmAlO_3 nanocrystalline powders by polymeric precursor method", *Applied Physics A*, 104, P. 465-469.
12. A.W. Coasts, J.P. Redfern (1963), "Thermogravimetric Analysis", A Review, *Analyst*, 88, P. 906-924.

13. C. Vijayakumar, H. Padma Kumar (2008), "Synthesis, characterization, sintering and dielectric properties of nanostructured perovskite-type oxide, $\text{Ba}_2\text{GdSbO}_6$ ", *Bulletin of Materials Science*, 31(5), P. 719–722.
14. Federico Locardi, Matilde Cirignano(2018), "Colloidal Synthesis of Double Perovskite $\text{Cs}_2\text{AgInCl}_6$ and Mn-doped $\text{Cs}_2\text{AgInCl}_6$ ", *Nanocrystals Journal of the American Chemical Society* P.1-8.
15. Y. Du, Z. X. Cheng (2011), "Magnetic and ferroelectric properties of multiferroic $\text{Bi}_2\text{NiMnO}_6$ nanoparticles", *Journal of Applied Physics* 109, P. 07B507.
16. Detlef M. Smilgiesa (2009), "Scherrer grain-size analysis adapted to grazing-incidence scattering with area detectors", *Journal of Applied Crystallography*, 42, P.1030-1034
17. Zhigang Zak Fang(2008), "Densification and Grain Growth During Sintering of Nanosized Particles", *International Materials Reviews* 53(6), P.326-352.
18. Gwang-Ho Kim (2010), "Effect of Oxide Dispersion on Dendritic Grain Growth Characteristics", *Materials Transactions*, 51(10) ,P. 1951 -1957.
19. Leila Firouzi Dalvand (2018), "Inhibitory Effect of Bismuth Oxide Nanoparticles Produced by *Bacillus licheniformis* on Methicillin-Resistant *Staphylococcus aureus* Strains", *Iranian J Biotech*, 16(4), P.e2102.
20. Arij Marzoukia, Hassen Harzalia (2016), "Optimization of the synthesis of multiferroic bismuth ferrite BiFeO_3 ", *Journal of the Tunisian Chemical Society*, 18, P. 38-42.
21. Andrew E. Smith(2009), " Mn^{3+} in Trigonal Bipyramidal Coordination: A New Blue Chromophore", *Journal of the American Chemical Society*, 131(47), P.17084-17086.
22. David W. Green (1979), "Matrix-isolated FeO, NiO, and CoO: Ground-state vibrational frequencies", *Journal of Molecular Spectroscopy*, 78(2), P.257-266.
23. Yi Du (2011), Magnetic and ferroelectric properties of multiferroic $\text{Bi}_2\text{NiMnO}_6$ nanoparticles, *Journal of Applied Physics*, 109 (7), P. 07B507-1-07B507-3.
24. Y. Du, Z. X. Cheng, X. L. Wanga (2011), Magnetic and ferroelectric properties of multiferroic $\text{Bi}_2\text{NiMnO}_6$ nanoparticles, *Journal of Applied Physics*, 109, P. 07B507.